Positronium atom scattering by H_2 in a coupled-channel framework

P K Biswas[$] and Sadhan K Adhikari[+]
[$]Departamento de Física-IGCE, Universidade Estadual Paulista
13500-970 Rio Claro, São Paulo, Brasil
[+]Instituto de Física Teórica, Universidade Estadual Paulista,
01405-900 São Paulo, São Paulo, Brasil

December 21, 2000

Abstract

The scattering of ortho positronium (Ps) by H_2 has been investigated using a three-Ps-state [Ps(1s,2s,2p)H_2(X $^1\Sigma_g^+$)] coupled-channel model and using Born approximation for higher excitations and ionization of Ps and B $^1\Sigma_u^+$ and b $^3\Sigma_u^+$ excitations of H_2. We employ a recently proposed time-reversal-symmetric nonlocal electron-exchange model potential. We present a calculational scheme for solving the body-frame fixed-nuclei coupled-channel scattering equations for Ps-H_2, which simplifies the numerical solution technique considerably. Ps ionization is found to have the leading contribution to target-elastic and all target-inelastic processes. The total cross sections at low and medium energies are in good agreement with experiment.

1 Introduction

With the availability of improved monoenergetic ortho positronium (Ps) beam, low-energy collision of exotic ortho Ps atom with neutral atoms and molecules is of interest in both physics and chemistry due to its vast applicational potential [1]. Recently, measurements of total ortho-Ps scattering cross section from various atomic and molecular targets (He, Ne, Ar, H_2, N_2, C_4H_{10}, and C_5H_{12}) have been carried out at low and medium to high energies [2, 3, 4]. Experimental investigations are also in progress for the measurement of pick-off annihilation of ortho Ps from closed shell atoms [5]. Because of the composite nature and high polarizability of Ps, a reliable theoretical description of Ps scattering is far more complicated than electron scattering [6], as excitations and ionization of Ps are expected to play a significant role for each target states. Besides if the target is vulnerable to excitations, prediction of total cross section becomes extremely difficult as the number of scattering channels grow as N^2, where N excited states of both Ps and target are considered.

Due to internal charge and mass symmetry, Ps atom yields zero elastic and even-parity transition potentials in the direct channel and Ps scattering is dominated mainly by exchange correlation [7, 8, 9]. This eventually complicates the convergence of a conventional coupled-channel description [7]. For Ps scattering with molecular target we have additional complication due to the presence of the nuclear degrees of freedom. The presence of three charge centers complicates the solution scheme of the coupled-channel equations. The degree of complication can be realized from the mathematical analysis of ref. [10] for Ps formation in positron-hydrogen-molecule scattering. Because of mathematical complication, this approach has not been further pursued in numerical analysis and there exists no successful calculation of Ps formation in positron-hydrogen-molecule scattering. We recall that the mathematical complication of a dynamical coupled-channel study of Ps formation in positron-hydrogen-molecule scattering is similar to that of Ps-H_2 scattering.

Here we undertake a theoretical study of Ps scattering by H_2. We employ a hybrid approach of treating the molecular orientational dependence as parameters in the coupled equations and then perform the partial-wave expansion [11]. The resulting one-dimensional equations are solved at the equilibrium nuclear separation by the matrix-inversion technique and the partial-wave cross sections are numerically averaged over molecular orientations. The present approach makes the Ps-H_2 scattering problem easily tractable.

Recently, we suggested a regularized electron-exchange model potential [6, 8] and demonstrated its effectiveness in exchange-dominated Ps scattering by performing quantum coupled-channel calculations using the ab initio framework of close-coupling method for both simple and complex targets [7, 12, 13, 14, 15]. In our initial calculations we used a nonsymmetric model-exchange potential for Ps scattering by H [12], He [8] and H_2 [6, 13] and obtained reasonably good agreement with experiment on He and H_2. In a subsequent application of Ps scattering by H, it was found that a time-reversal symmetric form of the exchange potential leads to far superior result than the nonsymmetric form both in qualitative and quantitative agreement with accurate variational calculations on H [7]. The symmetric potential also led to very good results for low-energy cross sections for Ps scattering by He, Ne, and Ar [16] in excellent agreement with experiment [4].

In view of the above we reinvestigate the problem of Ps scattering by H_2 using the symmetric exchange potential employing the three-Ps-state [Ps(1s,2s,2p)] coupled-channel model for elastic

and Ps(2s,2p) excitations. We solve the coupled-channel equations by the above scheme and report partial cross sections for Ps(1s,2s,2p) excitations. We also calculate cross sections for Ps excitations to $6 \geq n \geq 3$ states and Ps ionization using the first Born approximation. A target-elastic total cross section is calculated by adding the above partial cross sections. We use the present symmetric exchange potential to calculate the target-inelastic Born cross sections for excitation to B $^1\Sigma_u^+$ and b $^3\Sigma_u^+$ states of H_2 by Ps impact. We present a total Ps-H_2 cross section by adding the above target-elastic and target-inelastic results.

In section 2 we present the theoretical formulation in the body-frame fixed-nuclei approximation. In section 3 we present the numerical results. Finally, in section 4 we present a summary of our findings.

2 Theoretical Formulation

The total wave function Ψ of the Ps-H_2 system is expanded in terms of the Ps and H_2 quantum states as

$$\Psi(\mathbf{r_0}, \mathbf{r_1}, \mathbf{r_2}, \mathbf{x}; \mathbf{R}) \;=\; \mathcal{A} \sum_{a,b} \Big[F_{ab}(\mathbf{s_0}) \varphi_a(\mathbf{t_0}) \psi_b(\mathbf{r_1}, \mathbf{r_2}; \mathbf{R}) \Big] \tag{1}$$

where $\mathbf{s_0} = (\mathbf{x} + \mathbf{r_0})/2$, $\mathbf{t_0} = (\mathbf{x} - \mathbf{r_0})$, $\mathbf{x}$ ($\mathbf{r_0}$) is the coordinate of the positron (electron) of the Ps atom, $\mathbf{r_1}$ and $\mathbf{r_2}$ are the coordinates of the electrons of H_2, $2\mathbf{R}$ is the internuclear separation of H_2, φ_a the wave function of Ps, ψ_b the wave function of H_2, with b denoting the electronic configuration of H_2 and a denoting the quantum state of Ps. Here $\mathcal{A}$ denotes antisymmetrization with respect to Ps- and target-electron coordinates and F_{ab} is the continuum orbital of Ps with respect to the target. The spin of the positron is conserved in this process and the exchange profile of the Ps-target system is analogous to the corresponding electron-target system [14].

Primary complication arises in the coupled-channel study in retaining both the summations over Ps and target states in the coupling scheme. As we shall see later that the contribution of the individual target-inelastic channels to cross section is one order small compared to that of target-elastic channels. So we exclude the summation over target states from the coupling scheme and treat cross section for target excitations separately using Born approximation. In this work we are mostly interested to see whether the model can accommodate the measured total cross sections of Ps-H_2 scattering. So we retain the Ps(1s,2s,2p) excitations in the coupled-channel model and treat the remaining excitations by Born approximation. The first Born calculation with present regularized exchange leads to results reasonably close to coupled-channel calculation at medium energies. Hence it is expected that this calculation should yield a fairly good picture of the total cross section except near the Ps-excitation thresholds.

Projecting the resultant Schrödinger equation on the final Ps and target states and averaging over spin, the resulting momentum-space Lippmann-Schwinger scattering equation in the body-frame representation for a particular total electronic spin state S can be written as

$$f^S_{a'a}(\mathbf{k}', \mathbf{k}; \mathbf{R}) = \mathcal{B}^S_{a'a}(\mathbf{k}', \mathbf{k}; \mathbf{R}) - \frac{1}{2\pi^2} \sum_{a''} \int \mathrm{d}\mathbf{k}'' \frac{\mathcal{B}^S_{a'a''}(\mathbf{k}', \mathbf{k}''; \mathbf{R}) f^S_{a''a}(\mathbf{k}'', \mathbf{k}; \mathbf{R})}{k^2_{a''}/4 - k''^2/4 + \mathrm{i}0} \tag{2}$$

where $f^S_{a'a}$ are the scattering amplitudes, and $\mathcal{B}^S_{a'a}$ the corresponding Born potentials. $k_{a''}$ is the on-shell momentum of Ps in the intermediate channel a''. We use units $\hbar = m = 1$ where m

is the electronic mass. For Ps-H_2 target-elastic scattering there is only one scattering equation (2) corresponding to total electronic spin $S = 1/2$. The input potential of (2) is given by

$$\mathcal{B}^{1/2}_{a'a}(\mathbf{k}', \mathbf{k}; \mathbf{R}) = B^D_{a'a}(\mathbf{k}', \mathbf{k}; \mathbf{R}) - B^E_{a'a}(\mathbf{k}', \mathbf{k}; \mathbf{R}) \tag{3}$$

where B^D is the direct Born potential and B^E is the exchange potential. As in the ground electronic state $X^1\Sigma^+_g$ of H_2, the total electronic spin is zero, there will contribution of one target electron to $B^E_{a'a}(\mathbf{k}', \mathbf{k}; \mathbf{R})$ [17].

For the electronic ground state $X\ ^1\Sigma^+_g$ of H_2 we use the wave function of the form $\psi_b(\mathbf{r_1}, \mathbf{r_2}; \mathbf{R}) \equiv 1\sigma^{(b)}_g(1)1\sigma^{(b)}_g(2) = N^2 U_0(\mathbf{r_1}; \mathbf{R})U_0(\mathbf{r_2}; \mathbf{R})$, where $N = [2(1 + \mathcal{T})]^{-1/2}$ with $\mathcal{T}$ the overlap integral [18] and $U_0(\mathbf{r}; \mathbf{R}) = (\delta^3/\pi)^{1/2}[\exp(-\delta|\mathbf{r} - \mathbf{R}|) + \exp(-\delta|\mathbf{r} + \mathbf{R}|)]$ with $\delta = 1.166$ [18, 19]. For Ps we use the exact wave functions, e.g., for 1s state $\varphi(r) = \exp(-\beta r)/\sqrt{8\pi}$ with $\beta = 0.5$. For the excited states of H_2 we take the configurations $\psi_{b'}(\mathbf{r_1}, \mathbf{r_2}; \mathbf{R}) \equiv [1\sigma^{(b')}_g(1)1\sigma^{(b')}_u(2) \pm 1\sigma^{(b')}_g(2)1\sigma^{(b')}_u(1)]$, where $+$ $(-)$ corresponds to the spin singlet (triplet) state. All wave functions of H_2 are taken from ref. [19].

The direct Born potential for Ps transition from state a to a' and H_2 transition from b to b' can be rewritten in the following convenient factorized form [20]:

$$\begin{aligned}\mathcal{B}^D_{a'b'\leftarrow ab}(\mathbf{k_f}, \mathbf{k_i}; \mathbf{R}) &= \frac{4}{Q^2}\int d\mathbf{t}\varphi^*_{a'}(\mathbf{t})[e^{i\mathbf{Q}.\mathbf{t}/2} - e^{-i\mathbf{Q}.\mathbf{t}/2}]\varphi_a(\mathbf{t}) \\ &\times \int d\mathbf{r_1}d\mathbf{r_2}\psi^*_{b'}(\mathbf{r_1}, \mathbf{r_2}; \mathbf{R})\left[2\cos(\mathbf{Q}.\mathbf{R}) - \sum_{n=1}^{2} e^{i\mathbf{Q}.\mathbf{r_n}}\right]\psi_b(\mathbf{r_1}, \mathbf{r_2}; \mathbf{R}).\end{aligned} \tag{4}$$

Next we describe the electron-exchange model potential for Ps-H_2 scattering. We develop the model exchange potential from the following term [6, 13]:

$$\begin{aligned}\mathcal{B}^E_{a'b'\leftarrow ab}(\mathbf{k_f}, \mathbf{k_i}; \mathbf{R}) &= -\frac{1}{\pi}\int d\mathbf{x}d\mathbf{r}_0 d\mathbf{r_1}d\mathbf{r_2}e^{-i\mathbf{k_f}.(\mathbf{x}+\mathbf{r_1})/2}\varphi^*_{a'}(\mathbf{x} - \mathbf{r_1})\psi^*_{b'}(\mathbf{r_0}, \mathbf{r_2}; \mathbf{R})\frac{1}{|\mathbf{r_0} - \mathbf{r_1}|} \\ &\times \psi_b(\mathbf{r_1}, \mathbf{r_2}; \mathbf{R})\varphi_a(\mathbf{x} - \mathbf{r_0})e^{i\mathbf{k_i}.(\mathbf{x}+\mathbf{r_0})/2}.\end{aligned} \tag{5}$$

After removing the nonorthogonality of the initial and final wave functions of (5) and some straightforward simplification the model exchange potential for a general target-elastic transition becomes [6, 8]

$$\begin{aligned}\mathcal{B}^E_{a'b\leftarrow ab}(\mathbf{k_f}, \mathbf{k_i}; \mathbf{R}) &= \frac{4(-1)^{l+l'}}{(k_f^2 + k_i^2)/8 + (2\delta^2_{b(g)} + \beta_a^2 + \beta_{a'}^2)/2}\int d\mathbf{t}\varphi^*_{a'}(\mathbf{t})e^{i\mathbf{Q}.\mathbf{t}/2}\varphi_a(\mathbf{t}) \\ &\times \int d\mathbf{r_2}d\mathbf{r_0}\psi^*_b(\mathbf{r_0}, \mathbf{r_2}; \mathbf{R})e^{i\mathbf{Q}.\mathbf{r_0}}\psi_b(\mathbf{r_0}, \mathbf{r_2}; \mathbf{R}) \qquad (6) \\ &= \frac{4(-1)^{l+l'}}{(k_f^2 + k_i^2)/8 + (2\delta^2_{b(g)} + \beta_a^2 + \beta_{a'}^2)/2}\int d\mathbf{t}\varphi^*_{a'}(\mathbf{t})e^{i\mathbf{Q}.\mathbf{t}/2}\varphi_a(\mathbf{t}) \\ &\times \int d\mathbf{r_2}1\sigma^{(b)}_g(\mathbf{r_2})1\sigma^{(b)}_g(\mathbf{r_2})\int d\mathbf{r_0}1\sigma^{(b)}_g(\mathbf{r_0})e^{i\mathbf{Q}.\mathbf{r_0}}1\sigma^{(b)}_g(\mathbf{r_0}) \qquad (7)\end{aligned}$$

where l and l' are the angular momenta of the initial and final Ps states and $\mathbf{Q} = \mathbf{k_i} - \mathbf{k_f}$. Here $\delta_{b(g)}$ and β_a are the parameters of the H_2 and Ps wave functions in the initial state. The parameter $\beta^2_{a'}$ corresponds to the final-state binding energy of the Ps atom and is taken as

zero while considering exchange for the Ps ionization channel. For target-inelastic processes, following the prescription outlined in refs. [6, 8] the exchange potential takes the form

$$\begin{aligned}\mathcal{B}^{E}_{a'b'\leftarrow ab}(\mathbf{k_f},\mathbf{k_i};\mathbf{R}) &= \frac{4(-1)^{l+l'}}{(k_f^2+k_i^2)/8+(\delta^2_{b(g)}+\delta^2_{b'(u)}+\beta_a^2+\beta_{a'}^2)/2}\int d\mathbf{t}\varphi^*_{a'}(\mathbf{t})e^{i\mathbf{Q}.\mathbf{t}/2}\varphi_a(\mathbf{t}) \\ &\times \int d\mathbf{r_2}1\sigma_g^{(b')}(\mathbf{r_2})1\sigma_g^{(b)}(\mathbf{r_2})\int d\mathbf{r_0}1\sigma_u^{(b')}(\mathbf{r_0})e^{i\mathbf{Q}.\mathbf{r_0}}1\sigma_g^{(b)}(\mathbf{r_0}). \qquad (8)\end{aligned}$$

In (8) the additional indices b and b' are introduced on the molecular orbitals $1\sigma_g$ and $1\sigma_u$ to distinguish the initial and final states. The model exchange potentials (7) and (8) may be considered as a generalization of a similar potential suggested by Rudge [21] for electron-atom scattering. The nonlocal and time-reversal symmetric exchange potential (7) has a very convenient form and is expressed as a product of form factors of Ps and H_2. Both the direct and exchange amplitudes have been factored out in terms of Ps and target "form-factors" leading to a substantial simplification of the theoretical calculation. In our previous study of Ps-H_2 scattering [6, 13] the prefactor of the exchange potential was not time-reversal symmetric. In Eq. (7) we have restored time-reversal symmetry as in ref. [8] which is found to provide significant improvement in the results. Although, for electron-molecule scattering several model potentials are found in the literature [22, 23], there is no other convenient model exchange potential for Ps scattering.

3 Numerical Procedure and Results

In the body-frame calculation the coupled-channel equations are solved at the equilibrium nuclear separation $2R_0 = 1.4a_0$. The polar and azimuthal angles θ_R and ϕ_R of $\mathbf{R}$ are taken as parameters in the coupled equations [11]. This reduces (2) to the following form

$$f^{R_0,\theta_R,\phi_R}_{a'a}(\mathbf{k}',\mathbf{k}) = \mathcal{B}^{R_0,\theta_R,\phi_R}_{a'a}(\mathbf{k}',\mathbf{k}) - \frac{1}{2\pi^2}\sum_{a''}\int \mathrm{d}\mathbf{k}''\frac{\mathcal{B}^{R_0,\theta_R,\phi_R}_{a'a''}(\mathbf{k}',\mathbf{k}'')f^{R_0,\theta_R,\phi_R}_{a''a}(\mathbf{k}'',\mathbf{k})}{k^2_{a''}/4-k''^2/4+\mathrm{i}0}. \quad (9)$$

After standard partial-wave projection the three-dimensional coupled scattering equations (9) are first reduced to coupled one-dimensional integral equations in momentum space. The one-dimensional equations are then discretized by Gauss-Legendre quadrature rule and solved by the matrix inversion technique. A maximum of forty points are used in the discretization of the integrals. The discretized coupled-channel equations are solved for eight to ten discrete values each of polar and azimuthal angles θ_R and ϕ_R. This leads to a convergence of cross sections up to three significant figures. For targets with more charge asymmetry and for polar molecules we expect that more points will be required for angular averaging. The present averaging amounts to solving the coupled set of scattering equations sixty four to hundred times. Although this procedure increases the computational (CPU) time, mathematical complications of tedious (and untractable) angular-momentum analysis [10] are thus replaced by a tractable and convenient calculational scheme. Finally, the partial-wave cross sections are numerically averaged over molecular orientation using Gauss-Legendre quadrature points for both polar and azimuthal angles θ_R and ϕ_R. Maximum number of partial waves included in the calculation is 12. Contribution of higher partial waves to cross section is included by corresponding Born

terms. These Born cross sections are also numerically averaged over all molecular orientations in a similar fashion.

In figure 1, we show the angle-integrated target-elastic cross sections for elastic, Ps(2s+2p), Ps($3 \leq n \leq 6$) excitations and ionization of Ps. As expected and observed in previous calculations [7, 8, 12, 13] with other targets, the contribution of the Ps ionization channel to the cross section plays a dominant role from medium to high energies as can be seen in figure 1. The detailed angle-integrated partial cross sections of the Born and three-Ps-state calculation are tabulated in table 1. Near 10 eV, 20 eV and 30 eV the total Born cross sections for Ps(1s,2s,2p) are found to be nonconvergent by 28%, 9% and 4%, respectively. Near 10 eV, 20 eV and 30 eV the total Born cross sections for Ps($n = 2$) excitations are found to be nonconvergent by 18%, 6% and 3%, respectively. At 60 eV the Born and three-Ps-state results are essentially identical. The nonconvergence of Ps($n \geq 3$) excitations calculated using Born approximation are expected to lie within the limit set by Ps($n = 2$) cross sections above. It is expected from experience that the ionization cross section calculated using Coulomb Born will be more converged than the Ps($n = 2$) Born cross sections.

Table 1: Ps-H_2 partial cross sections in units of πa_0^2 at different positronium energies using the Born approximation and three-Ps-state calculation

E (eV)	Ps(1s) Born	Ps(1s) 3-St	Ps(2s) Born	Ps(2s) 3-St	Ps(2p) Born	Ps(2p) 3-St	Ps($n \geq 3$) Born	Ps-ion Born
0.068	23.72	3.79						
0.612	17.56	3.16						
1.45	11.84	2.47						
3	6.71	1.60						
4	5.03	1.17						
5	3.94	0.81						
6	3.18	1.01	0.098	0.23	3.46	2.28	0	0
7	2.63	1.05	0.101	0.18	3.60	2.52	1.28	0.11
8	2.22	1.03	0.092	0.14	3.36	2.51	1.43	1.15
10	1.65	0.94	0.072	0.090	2.80	2.27	1.29	3.03
12.5	1.21	0.81	0.052	0.068	2.24	1.93	1.05	4.34
15	0.92	0.68	0.041	0.054	1.85	1.65	0.87	4.94
20	0.59	0.49	0.026	0.035	1.34	1.25	0.63	5.18
25	0.40	0.36	0.017	0.023	1.04	0.99	0.49	4.93
30	0.29	0.27	0.012	0.017	0.84	0.81	0.40	4.55
40	0.17	0.16	0.007	0.009	0.60	0.58	0.28	3.80
60	0.07	0.07	0.003	0.004	0.37	0.37	0.17	2.72

Now we concentrate on some target inelastic processes. Each target inelastic transition is accompanied by elastic, excitation and ionization of Ps and hence by an infinite number of possibilities. Here to account for target inelastic processes we consider Ps($n = 1 \rightarrow 6$) discrete excitations and ionization of Ps using the first Born approximation. Contribution of higher discrete excitations of Ps are expected to be insignificant and are neglected in the calculation. We calculate the cross sections for the inelastic transition Ps(1s) + H_2(X $^1\Sigma_g^+$) $\rightarrow$ Ps* + H_2 (B $^1\Sigma_u^+$) where Ps* represents the ground and the excited states of the Ps atom. These Born cross

sections are also calculated at a equilibrium internuclear separation $2R_0 = 1.4a_0$ and finally averaged over angular orientations of the target. In figure 2 we display the Born contribution of partial cross sections for transition to different Ps states while the hydrogen molecule is excited to the H_2 (B $^1\Sigma_u^+$) state. The total cross section summing the different contributions is also shown for this target-inelastic process. When compared with the corresponding total cross section calculated with the nonsymmetric exchange potential [6] (not shown in figure 2) we find marginal change at low energies (below 20 eV) and basically no change at medium to high energies. This is quite expected as the effect of exchange dies out at higher energies and these cross sections are controlled by the direct Born potentials.

Next we calculate the cross sections for the inelastic transition Ps(1s) + H_2(X $^1\Sigma_g^+$) $\rightarrow$ Ps* + H_2(b $^3\Sigma_u^+$) using the first Born approximation, where Ps* represents the ground and the abovementioned excited states of the Ps atom. These cross sections are again calculated for equilibrium internuclear separation $2R_0 = 1.4a_0$ and averaged over molecular orientations. In figure 3 we display the contribution of partial cross sections for transition to different Ps states while the hydrogen molecule is excited to the H_2 (b $^3\Sigma_u^+$) state. The total cross section summing the different contributions is also shown for this target-inelastic process. There is significant change when we compare this total cross section calculated with the symmetric exchange potential with our previous result [6] obtained with the nonsymmetric exchange potential. This is quite expected as this process is purely exchange dominated. The qualitative and quantitative differences between the two total cross sections reveal the importance of using the symmetric exchange potential.

In figure 4, we exhibit the total cross section obtained from target-elastic processes (Ps excitation up to $n = 6$ and Ps ionization) plus target excitations to B $^1\Sigma_u^+$ and b $^3\Sigma_u^+$ states [6, 13] and compare with the total cross section measurements of ortho-Ps scattering from H_2 [2, 4]. The agreement with the experimental cross sections is highly encouraging. Here, we have considered only two lowest target-inelastic processes and their combined effect on the total cross section. This gives an indication that the inclusion of remaining important target-inelastic cross sections might give a better agreement with measurement.

However, the present theoretical peak in total cross section is shifted to a lower energy compared to experiment. This trend was also found in our calculation of Ps-He scattering [7]. In the energy range of 7 to 15 eV, the total cross section overestimates the measured data. This is due to the fact that Ps($n \geq 3$) excitations and ionization have been treated in the first Born approximation framework. The neglect of other target-inelastic channels and the first Born calculation for higher excitations and, in particular, ionization of Ps are supposed to be responsible for the shift in the theoretical peak. A dynamical calculation for higher Ps excitations and ionization should reduce the theoretical total cross section in the intermediate energy region, while the inclusion of further target-inelastic channels will increase the cross section for medium to higher energies. These two effects are expected to shift the peak in the total cross section to higher energies and lead to a better agreement with experiment.

A previous first Born description of Ps-H_2 scattering [24] with Born-Oppenheimer exchange [25] led to unphysically large cross section at low energies. The poor performance of that scheme in Ps scattering compared to electron scattering is due to the fact that in the absence of the direct potential (zero for elastic scattering), the Born-Oppenheimer exchange potential solely determines the cross section. This clearly shows the very unrealistic nature of the Born-Oppenheimer exchange potential at low energies.

In previous studies [7, 8, 14] of Ps scattering we introduced a parameter C in the exchange potential for obtaining a more quantitative fit with experiment essentially by replacing the denominator term in (7) by $(k_f^2 + k_i^2)/8 + C(\delta_a^2 + \delta_{a'}^2 + \beta_b^2 + \beta_{b'}^2)/2$. In the original form the constant $C = 1$ and we have used this value in this study. However, it can be varied slightly from unity to obtain a precise fit of a low-energy scattering observable (experimental or variational), as has been done in some applications of model potentials [23]. A variation of C from unity leads to a variation of the average values for square of momenta [8, 12], which were taken as the binding energy parameters (δ^2, β^2 etc.) in the expression for the denominator in (7). This variation, in turn, tunes the strength of the exchange potential at low energies. At high energies this model potential is insensitive to this parametrization and leads to the well-known Born-Oppenheimer form of exchange [25].

4 Summary

To summarize, we have used a time-reversal symmetric form of the nonlocal model potential for exchange and applied it to the study of Ps-H_2 scattering. We have also presented a simplified prescription for performing coupled-channel dynamical scattering calculation with molecular target using a body-frame fixed-nuclei scheme. With this prescription we have performed a three-Ps-state coupled-channel calculation of target-elastic Ps-H_2 scattering. Higher excitations and ionization of the Ps atom are treated using the first Born approximation with a regularized exchange. We also calculated cross sections for two target-inelastic excitations of H_2 (B $^1\Sigma_u^+$ and b $^3\Sigma_u^+$) using first Born approximation with present exchange considering Ps excitations ($n = 1, ..., 6$) and ionization. Considering the fact that we have considered only two target-inelastic processes, the present total cross section is in encouraging agreement with experiment. The tractability of of the present dynamical calculational scheme for molecular targets and the success of the present time-reversal symmetric electron-exchange potential in describing Ps-H_2 scattering should stimulate further investigation with both.

We thank the Conselho Nacional de Desenvolvimento Científico e Tecnológico, Fundação de Amparo à Pesquisa do Estado de São Paulo, and Financiadora de Estudos e Projetos of Brazil for partial financial support.

References

[1] Charlton M and Laricchia G 1991 *Comments At. Mol. Phys.* **26** 253
Charlton M and Laricchia G 1990 *J. Phys. B: At. Mol. Opt. Phys.* **23** 1045
Gidley D W, Rich A and Zitzewitz P W 1982 *Positron Annihilation, Eds. Coleman P G, Sharma S C and Diana L M* (Amsterdam: North-Holland) pp 11
Tang S and Surko C M 1993 *Phys. Rev. A* **47** R743

[2] Garner A J, Laricchia G and Ozen A 1996 *J. Phys. B: At. Mol. Opt. Phys.* **29** 5961

[3] Garner A J and Laricchia G 1996 *Can. J. Phys.* **74** 518
Nagashima Y, Hyodo T, Fujiwara K and Ichimura A 1998 *J. Phys. B: At. Mol. Opt. Phys.* **31** 329
Zafar N, Laricchia G, Charlton M and Garner A 1996 *Phys. Rev. Lett.* **76** 1595

Laricchia G 1995 *Nucl. Instrum. Methods Phys. Res. B* **99** 363
Laricchia G 1996 *Hyperfine Interact.* **100** 71

[4] Skalsey M, Engbrecht J J, Bithell R K, Vallery R S and Gidley D W 1998 *Phys. Rev. Lett.* **80** 3727

[5] Gidley D W 1999 *private communication*
Hyodo T 1999 *private communication*

[6] Biswas P K and Adhikari S K 1998 *J. Phys. B: At. Mol. Opt. Phys.* **31** L315

[7] Adhikari S K and Biswas P K 1999 *Phys. Rev. A* **59** 2058

[8] Biswas P K and Adhikari S K 1999 *Phys. Rev. A* **59** 363

[9] Adhikari S K, Biswas P K and Sultanov R 1999 *Phys. Rev. A* **59** 4824

[10] Mukherjee T and Ghosh A S 1991 *J. Phys. B: At. Mol. Opt. Phys.* **24** L193

[11] Lane N F 1980 *Rev. Mod. Phys.* **52** 29
Hara S 1969 *J. Phys. Soc. Jpn.* **27** 1009, 1592
Temkin A 1976 *Comments At. Mol. Phys.* **5** 55
Herzenberg A and Mandl F 1962 *Proc. R. Soc. London A* **270** 48

[12] Biswas P K and Adhikari S K 1998 *J. Phys. B: At. Mol. Opt. Phys.* **31** 3147 and 5403

[13] Biswas P K and Adhikari S K 1998 *J. Phys. B: At. Mol. Opt. Phys.* **31** L737

[14] Biswas P K and Adhikari S K 2000 *Chem. Phys. Lett.* **317** 129

[15] Ray H 1999 *J. Phys. B: At. Mol. Opt. Phys.* **32** 5681
Ray H 1999 *Phys. Lett. A* **252** 316

[16] Frolov A M and Smith Jr. V H 1997 *Phys. Rev. A* **55** 2662
Ho Y K 1986 *Phys. Rev. A* **34** 609
Ho Y K 1978 *Phys. Rev. A* **17** 1675

[17] Riley M E and Truhlar D G 1975 *J. Chem. Phys.* **63** 2182

[18] Biswas P K, Mukherjee T and Ghosh A S 1991 *J. Phys. B: At. Mol. Opt. Phys.* **24** 2601

[19] Mulliken R S and Ermler W C 1977 *Diatomic Molecules Results of ab Initio Calculations* (New York: Academic) pp 44 - 47

[20] Biswas P K and Ghosh A S 1996 *Phys. Lett. A* **223** 173

[21] Rudge M R H 1965 *Proc. Phys. Soc.* **86** 763
Ochkur V I 1964 *Sov. Phys. − JETP* **18** 503

[22] Fliflet A W and McKoy V 1980 *Phys. Rev. A* **21** 1863
Lima M A P, Gibson T L, Huo W M and McKoy V 1985 *J. Phys. B: At. Mol. Opt. Phys.* **18** L865
Baille P and Darewych J W 1977 *J. Phys. B: At. Mol. Opt. Phys.* **10** L615
Baluja K L, Noble C J and Tennyson J 1985 *J. Phys. B: At. Mol. Opt. Phys.* **18** L851
Lee M-T, Fujimoto M M, Kroin T and Iga I 1996 *J. Phys. B: At. Mol. Opt. Phys.* **29** L425
Chung S and Lin C C 1978 *Phys. Rev. A* **17** 1874

[23] Morrison M A, Feldt A N and Austin D 1984 *Phys. Rev. A* **29** 2518
Gibson T L and Morrison M A (1982) *J. Phys. B: At. Mol. Opt. Phys.* **15** L221.

[24] Comi M, Prosperi G M and Zecca A 1983 *Nuovo Cimento* **2** 1347

[25] Oppenheimer J R *Phys. Rev.* **32** 361.

Figure Caption:

1. Angle integrated target-elastic Ps-H_2 partial cross sections at different positronium energies: elastic (solid line) and Ps(2s+2p) excitation (dashed-dotted line) from three-state coupled-channel model at low energies interpolated to exchange Born at high energies, Ps($6 \geq n \geq 3$) excitation (dashed-double-dotted line), Ps ionization (dashed line) from exchange Born.

2. Angle integrated target-inelastic Ps-H_2 partial and total cross sections at different positronium energies to H_2 (B $^1\Sigma_u^+$) state using the first Born approximation: Ps(1s) (dashed-dotted line), Ps(2s+2p) (dashed-double-dotted line), Ps($6 > n > 2$) excitation (dotted line), Ps ionization (dashed line), and total (full line).

3. Angle integrated target-inelastic Ps-H_2 partial and total cross sections at different positronium energies to H_2 (b $^3\Sigma_u^+$) state using the first Born approximation: Ps(1s) (dashed-dotted line), Ps(2s+2p) (dashed-double-dotted line), Ps($6 > n > 2$) excitation (dotted line), Ps ionization (dashed line), total (full line), total cross section with the nonsymmetric potential from ref. [6] (dashed-triple-dotted line).

4. Total Ps-H_2 cross section at different positronium energies: total target elastic cross section from figure 1 (dashed line), total target-elastic (from figure 1) plus target-inelastic (from figures 2 and 3) cross section (solid line), experimental data (solid circles from ref. [2], solid square from ref. [4]).

Figure 1

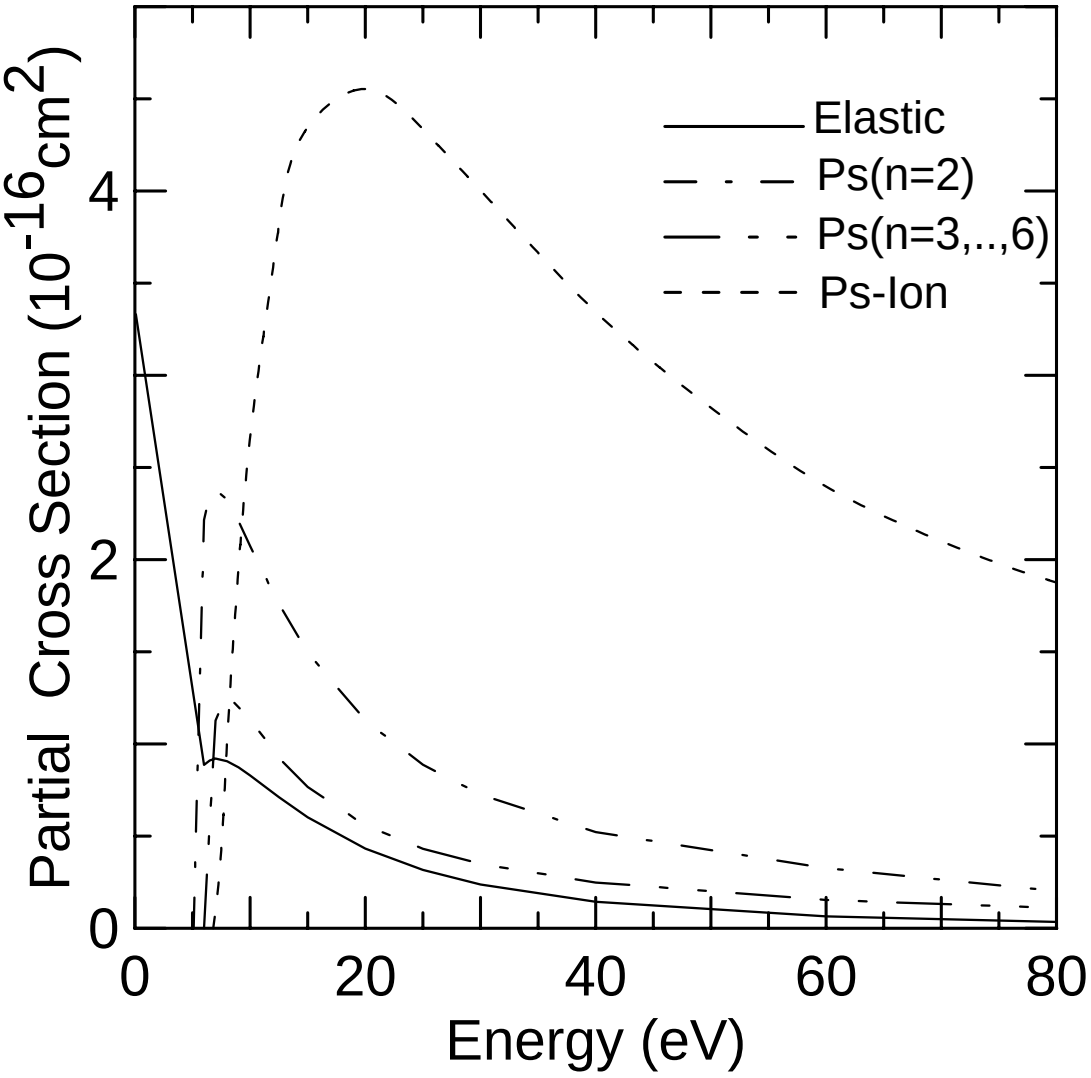
Partial Cross Section (10^{-16}cm^2)
Energy (eV)
Elastic
Ps(n=2)
Ps(n=3,..,6)
Ps-Ion
0
2
4
0
20
40
60
80

Figure 2

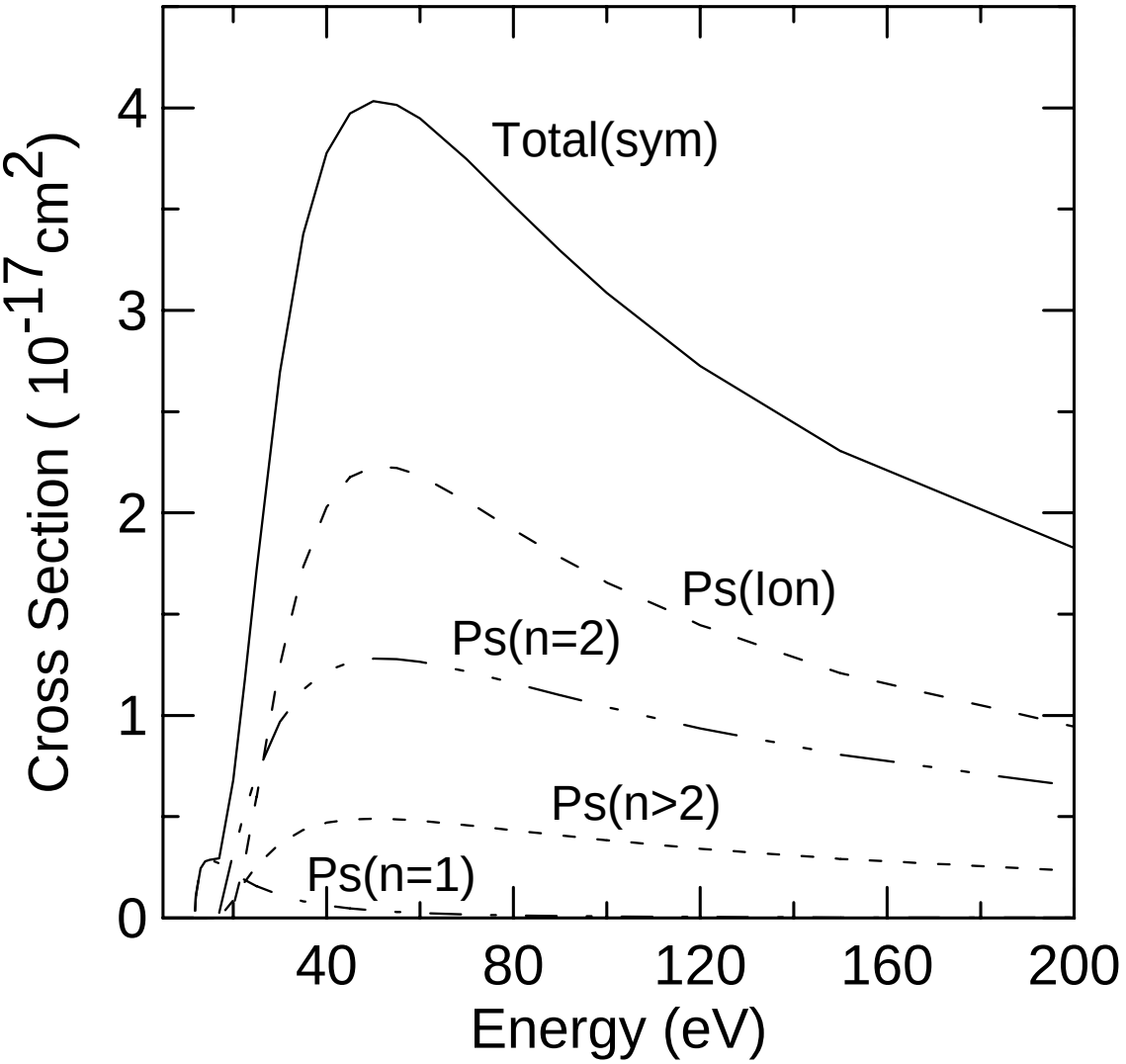
Total(sym)
Ps(Ion)
Ps(n=2)
Ps(n>2)
Ps(n=1)
Cross Section (10-17cm2)
Energy (eV)
0
1
2
3
4
40
80
120
160
200

Figure 3

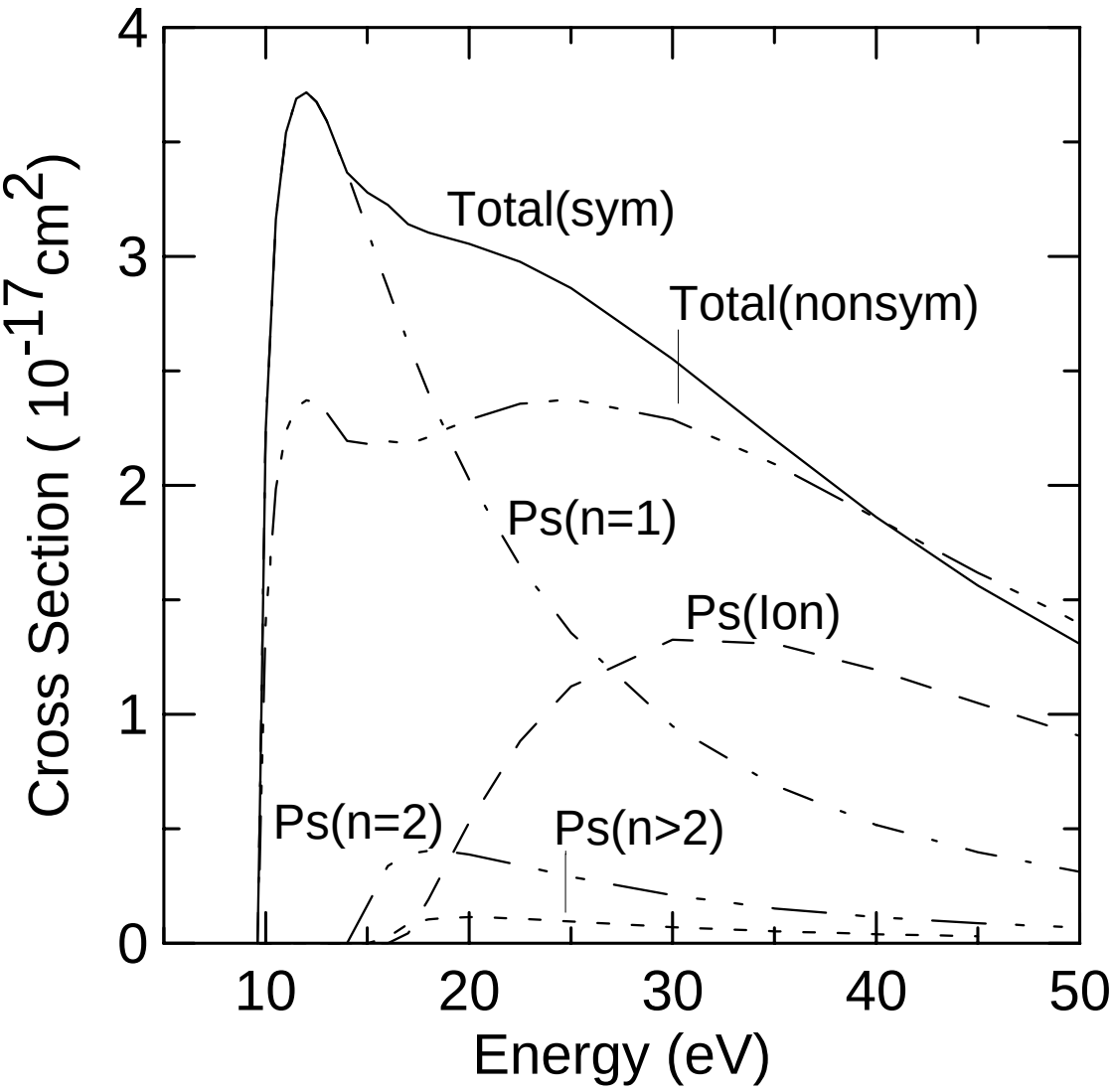
Cross Section (10-17cm2)
Energy (eV)
Total(sym)
Total(nonsym)
Ps(n=1)
Ps(Ion)
Ps(n=2)
Ps(n>2)
0
1
2
3
4
10
20
30
40
50

Figure 4